Available online at www.elixirpublishers.com (Elixir International Journal)

Applied Mathematics

Elixir Appl. Math. 83 (2015) 32834-32845

ISSN: 2229-712X

Mixed convective flow in a vertical channel filled with porous and fluid layer using boundary conditions of third kind

J. Prathap Kumar, J.C. Umavathi and Y. Ramarao

Department of Mathematics, Gulbarga University, Kalaburagi-585 106, Karnataka, India.

ARTICLE INFO

Article history:

Received: 19 April 2015;

Received in revised form:

25 May 2015;

Accepted: 1 June 2015;

Keywords

Mixed convection, Brinkman model, Immiscible fluids,
Porous medium,
Differential Transform Method,
Boundary condition of third kind.

ABSTRACT

Combined free and forced convection flow in a vertical channel filled with porous and fluid layer is studied with boundary conditions of third kind. The flow is modeled using Brinkman model. The viscous and Darcy dissipation terms are also included in the energy equation. The plate exchanges heat with an external fluid. Separate solutions are matched at the interface using suitable matching conditions. The coupled non-linear governing equations are solved using perturbation series method valid for small values of the perturbation parameter. The condition for perturbation parameter is relaxed by finding the solutions of the governing equations using Differential Transform method. The effects of various parameters on the flow such as mixed convection parameter, porous parameter, viscosity ratio, width ratio, conductivity ratio and Biot numbers on the flow are explored graphically. Further it is also shown that the Differential Transform method solutions agree very well with perturbation method series solutions for small values of the perturbation parameter.

Introduction

Mixed convection flow in a vertical duct maintained at different constant temperatures constitutes a bench mark configuration. Solar heat storage systems and crystal growth are salient engineering examples of convection problems (Ostrach, [1], Langlois, [2], and Schwabe, [3]). The majority of existing research has been principally devoted to the case of filling the entire enclosure in realistic situations. However, the fluid systems often times consists of two separate, immiscible liquids. Sparrow et al. [4] performed a symmetrically organized experiment in a square cavity using a layer of Hexa-Decade overlaying a layer of water. Kimura et al. [5] by using a spindle oil-Ethylene glycol combination and a spindle oil-water combination examined the effects of the ratio of depths of two layers on the overall Nusselt numbers.

Mixed convective heat transfer in porous media has been a subject of continuing interest during past decades. This interest is due to the wide range of applicability of heat transfer processes in porous media, such as energy storage units, heating pipes and catalytic reactors. Fluid flow and heat transfer characteristics at the interface region in systems which consists of a fluid-saturated porous medium and an adjacent horizontal fluid layer have received considerable attention. This is due to the fact that this type of problems stems from the wide range of engineering applications such as electronic cooling, drying process, thermal insulation, crude oil extraction and geothermal engineering.

A thorough understanding of fluid mechanics and heat transfer characteristics in porous media is quite complicated. The study of the fluid flow boundary conditions at the interface region was one of the first attempts of Beavers and Joseph [6]. A slip in the velocity at the interface was detected by them after performing a series of experiments. One of the earlier attempts regarding this type of boundary condition in porous medium was presented by Neale and Nadar [7]. In this study, the authors proposed continuity in both the velocity and the velocity gradient at the interface by introducing the Brinkman term in the momentum equation for the porous side. Vafai and Kim [8] considered the shear stress in the fluid and the porous medium to be equal at the interface region. Vafai and Thiyagaraja [9] considered continuity of shear stress and heat flux at the interface for the non-Darcy model. Following the analysis of Vafai and Thiyagaraja [9], Malashetty et al. [10, 11], Umavathi et al. [12-16] and Prathap Kumar et al. [17-18] studied convective heat transfer in a composite porous medium.

Recent technological implications have given rise to increased interest in combined free and forced convection flow in vertical channels in which the objective is to secure the quantitative understanding of the configuration having current engineering applications. Al-Hadharami et al. [19], and Param and Keyhani [20] studied fully developed buoyancy-assisted mixed convection in a vertical annulus by using the Brinkman-extended Darcy model. Their results indicated that the Brinkman term could be neglected for lower Darcy numbers. Murulidhar [21] performed a numerical calculation for buoyancy-assisted mixed convection in a vertical annulus by using Darcy model. Analytical Taylor series solutions have been reported for the mixed convection in a vertical channel for isoflux-isothermal wall conditions by Barletta et al. [22]. The same approach has been applied to the mixed convection channel flow of clear fluids for the case of symmetrical isothermal-isothermal wall conditions by Barletta et al. [23]. In the past, the laminar forced convection heat transfer in the thermal entrance region of a rectangular channel has been analyzed either for the temperature boundary conditions of the first kind, characterized by prescribed wall temperature (Wibulswas, [24], Lyczkowski et al., [25], and Javeri, [26]) or for the boundary conditions of the second kind, expressed by the prescribed wall heat flux (Hicken, [27], Sparrow and Siegel, [28]). Zanchini, [29] analyzed the effects of viscous dissipation on mixed convection in a vertical channel with boundary conditions of third kind. Recently Umavathi and Santhosh [30, 31] and Umavathi et al. [32, 33] studied mixed convection in a vertical channel with boundary conditions of third kind.

Tele:
E-mail addresses: p_rathap@yahoo.com

A popular analytic method frequently employed in fluid dynamics is the perturbation method (Rashidi and Ganji, [34]). Numerical methods such as the Runge-Kutta method and finite difference techniques (Bĕg et al., [35]) are based on discretization techniques, and they permit computation of only approximate solutions for some values of the time and space variables. However, both numerical and perturbation methods themselves fail to yield a simple method for adjusting or controlling the convergence region and rate of a given approximate series. To overcome this difficulty, Zhou [36] employed the basic ideas of the differential transform method (DTM) for ordinary differential equations. The main advantage of DTM is that without requiring linearization, discretization, or perturbation techniques, it can be applied directly to non-linear differential equations Another important advantage is that this method is capable of greatly reducing the size of computational work while still accurately providing the series solution with fast convergence rate. This method is well addressed in Yeh et al., [37], Ravi Kanth and Aruna, [38], Abdel-Halim Hassan, [39], Rashidi, [40], Yaghoobi and Torabi, [41] and Rashidi et al., [42].

In this article, a detailed analytical and semi-analytical investigation of the steady mixed convection in a vertical channel filled with composite porous medium with boundary conditions of third kind is presented. The flow in the porous medium is the non-Darcy model. Both equal and different reference temperatures of the external fluid, as well as both equal and different Biot numbers are considered.

Mathematical Formulation

The geometry under consideration illustrated in Fig. 1 consists of two infinite parallel plates extending in the X and Z directions. The region $-h_1/2 \le Y \le 0$ is occupied by a permeable fluid with permeability κ, density ρ_1, viscosity μ_1, thermal conductivity k_1, and thermal expansion coefficient β_1, and the region $0 \le Y \le h_2/2$ is occupied by a purely viscous, incompressible fluid of density ρ_2, viscosity μ_2, thermal conductivity k_2, and thermal expansion coefficient β_2. The fluids are assumed to have constant properties except the density in the buoyancy term in the momentum equation $\rho_1 = \rho_0\left[1-\beta_1\left(T_1-T_0\right)\right]$ and $\rho_2 = \rho_0\left[1-\beta_2\left(T_2-T_0\right)\right]$. A fluid rises in the channel driven by buoyancy forces. The transport properties of both fluids are assumed to be constant.

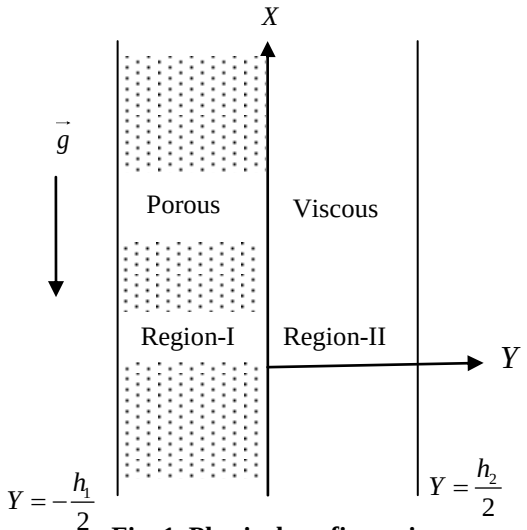

Fig. 1. Physical configuration

We consider the fluids to be incompressible and the flow is steady, laminar, and fully developed. It is assumed that the only non-zero component of the velocity $\vec{q}$ is the X-component $U_i(i=1,2)$. Thus, as a consequence of the mass balance equation, one obtains

$$\frac{\partial U_i}{\partial X} = 0 \tag{1}$$

so that U_i depends only on Y. The stream wise and the transverse momentum balance equations yields

Region-I

$$g\beta_1\left(T_1-T_0\right) - \frac{1}{\rho_1}\frac{\partial P}{\partial X} + \nu_1\frac{d^2U_1}{dY^2} - \frac{\nu_1}{\kappa}U_1 = 0 \tag{2}$$

Region-II

$$g\beta_2\left(T_2-T_0\right) - \frac{1}{\rho_2}\frac{\partial P}{\partial X} + \nu_2\frac{d^2U_2}{dY^2} = 0 \tag{3}$$

The Y-momentum balance equation in both the regions can be expressed as

$$\frac{\partial P}{\partial Y} = 0 \tag{4}$$

where $P = p + \rho_0 gX$ (assuming $p_1 = p_2 = p$) is the difference between the pressure and hydrostatic pressure. On account of Eq. 4, p depends only on X so that Eqs. 2 and 3 can be rewritten as

Region-I

$$T_1 - T_0 = \frac{1}{g\beta_1\rho_1}\frac{dP}{dX} - \frac{\nu_1}{g\beta_1}\frac{d^2U_1}{dY^2} + \frac{\nu_1}{g\beta_1\kappa}U_1 \tag{5}$$

Region-II

$$T_2 - T_0 = \frac{1}{g\beta_2\rho_2}\frac{dP}{dX} - \frac{\nu_2}{g\beta_2}\frac{d^2U_2}{dY^2} \tag{6}$$

From Eqs. 5 and 6 one obtains

Region-I

$$\frac{\partial T_1}{\partial X} = \frac{1}{g\beta_1\rho_1}\frac{d^2P}{dX^2} \tag{7}$$

$$\frac{\partial T_1}{\partial Y} = -\frac{\nu_1}{g\beta_1}\frac{d^3U_1}{dY^3} + \frac{\nu_1}{g\beta_1\kappa}\frac{dU_1}{dY} \tag{8}$$

$$\frac{\partial^2 T_1}{\partial Y^2} = -\frac{\nu_1}{g\beta_1}\frac{d^4U_1}{dY^4} + \frac{\nu_1}{g\beta_1\kappa}\frac{d^2U_1}{dY^2} \tag{9}$$

Region-II

$$\frac{\partial T_2}{\partial X} = \frac{1}{g\beta_2\rho_2}\frac{d^2P}{dX^2} \tag{10}$$

$$\frac{\partial T_2}{\partial Y} = -\frac{\nu_2}{g\beta_2}\frac{d^3U_2}{dY^3} \tag{11}$$

$$\frac{\partial^2 T_2}{\partial Y^2} = -\frac{\nu_2}{g\beta_2}\frac{d^4U_2}{dY^4} \tag{12}$$

Both the walls of the channel will be assumed to have a negligible thickness and to exchange heat by convection with an external fluid. In particular, at $Y = -h_1/2$ the external convection coefficient will be considered as uniform with the value q_1 and the fluid in the region $-h_1/2 \le Y \le 0$ will be assumed to have a uniform reference temperature T_{q_1}. At $Y = h_2/2$ the external convection coefficient will be considered as uniform with the value q_2 and the fluid in the region

$0 \le Y \le h_2/2$ will be supposed to have a uniform reference temperature $T_{q_2} \ge T_{q_1}$. Therefore, the boundary conditions on the temperature field can be expressed as

$$-k_1 \left.\frac{\partial T_1}{\partial Y}\right|_{Y=-\frac{h_1}{2}} = q_1\left[T_{q_1} - T_1\left(X,-h_1/2\right)\right] \tag{13}$$

$$-k_2 \left.\frac{\partial T_2}{\partial Y}\right|_{Y=\frac{h_2}{2}} = q_2\left[T_2\left(X,h_2/2\right) - T_{q_2}\right] \tag{14}$$

On account of Eqs. 8 and 11, Eqs. 13 and 14 can be rewritten as

$$\left.\frac{d^3U_1}{dY^3}\right|_{Y=-\frac{h_1}{2}} - \frac{1}{\kappa}\left.\frac{dU_1}{dY}\right|_{Y=-\frac{h_1}{2}} = \frac{g\beta_1}{k_1\nu_1} q_1\left(T_{q_1} - T_1\left(X,-h_1/2\right)\right) \tag{15}$$

$$\left.\frac{d^3U_2}{dY^3}\right|_{Y=\frac{h_2}{2}} = \frac{g\beta_2}{k_2\nu_2} q_2\left[T_2\left(X,h_2/2\right) - T_{q_2}\right] \tag{16}$$

On account of Eqs. 5 and 6 there exist a constant A such that

$$\frac{dP}{dX} = A \tag{17}$$

For the problem under examination, the energy balance equation in the presence of viscous dissipation can be written as

Region-I

$$\frac{d^2T_1}{\partial Y^2} = -\frac{\nu_1}{\alpha_1 C_p}\left(\frac{dU_1}{dY}\right)^2 - \frac{\nu_1}{C_p\kappa\alpha_1}U_1^2 \tag{18}$$

Region-II

$$\frac{d^2T_2}{\partial Y^2} = -\frac{\nu_2}{\alpha_2 C_p}\left(\frac{dU_2}{dY}\right)^2 \tag{19}$$

From Eqs. 9 and 18, Eqs.12 and 19 allow one to obtain differential equations for U_i namely

Region-I

$$\frac{d^4U_1}{dY^4} = g\beta_1\left(\frac{1}{g\beta_1\kappa}\frac{d^2U_1}{dY^2} + \frac{1}{c_p\alpha_1}\left(\frac{dU_1}{dY}\right)^2 + \frac{U_1^2}{c_p\kappa\alpha_1}\right) \tag{20}$$

Region-II

$$\frac{d^4U_2}{dY^4} = \frac{g\beta_2}{\alpha_2 C_p}\left(\frac{dU_2}{dY}\right)^2 \tag{21}$$

The boundary conditions on velocity are no-slip conditions, and those induced by boundary conditions on temperature. In addition, the continuity of velocity, shear stress, temperature and heat flux at the interface between the two layers are assumed as:

$$U_1\left(-h_1/2\right) = U_2\left(h_2/2\right) = 0 \tag{22}$$

together with Eqs. 15 and 16, which on account of Eqs. 5 and 6 can be rewritten as

$$\frac{d^3U_1}{dY^3} - \frac{1}{\kappa}\frac{dU_1}{dY} - \frac{q_1}{k_1}\frac{d^2U_1}{dY^2} = \frac{q_1}{k_1}\frac{g\beta_1}{\nu_1}\left[T_{q_1} - T_0\right] - \frac{q_1}{k_1}\frac{A}{\mu_1}$$

at $Y = -\frac{h_1}{2}$

$$\frac{d^3U_2}{dY^3} + \frac{q_2}{k_2}\frac{d^2U_2}{dY^2} = \frac{Aq_2}{\mu_2 k_2} - \frac{g\beta_2 q_2}{\nu_2 k_2}\left[T_{q_2} - T_0\right] \text{ at } Y = \frac{h_1}{2} \tag{23}$$

$$U_1(0) = U_2(0)$$

$$\mu_1\frac{dU_1}{dY} = \mu_2\frac{dU_2}{dY} \text{ at } Y = 0$$

$$T_1(0) = T_2(0)$$

$$k_1\frac{dT_1}{dY} = k_2\frac{dT_2}{dY} \text{ at } Y = 0 \tag{24}$$

Equations 20-24 determine the velocity distribution. They can be written in a dimensionless form by means of the following dimensionless parameters:

$$u_1 = \frac{U_1}{U_0^{(1)}};\ u_2 = \frac{U_2}{U_0^{(2)}};\ y_1 = \frac{Y_1}{D_1};\ y_2 = \frac{Y_2}{D_2};\ Gr = \frac{g\beta_1\Delta T D_1^3}{\nu_1^2};$$

$$\mathrm{Re} = \frac{U_0^{(1)}D_1}{\nu_1};\ Br = \frac{U_0^{(1)^2}\mu_1}{k_1\Delta T};\ \Lambda = \frac{Gr}{\mathrm{Re}};\ \theta_1 = \frac{T_1 - T_0}{\Delta T};\ \theta_2 = \frac{T_2 - T_0}{\Delta T}$$

$$R_T = \frac{T_2 - T_1}{\Delta T};\ \sigma = \frac{D_1}{\sqrt{\kappa}};\ Bi_1 = \frac{h_1 D_1}{k_1};\ Bi_2 = \frac{h_2 D_2}{k_2};$$

$$s = \frac{Bi_1 Bi_2}{Bi_1 Bi_2 + 2Bi_1 + 2Bi_2} \tag{25}$$

where $D_i = 2h_i$ is the hydraulic diameter. The reference velocity and the reference temperature are given by

$$U_0^{(1)} = -\frac{AD_1^2}{48\mu_1},\ U_0^{(2)} = -\frac{AD_2^2}{48\mu_2},$$

$$T_0 = \frac{T_{q_1} + T_{q_2}}{2} + s\left(\frac{1}{Bi_1} - \frac{1}{Bi_2}\right)\left(T_{q_2} - T_{q_1}\right) \tag{26}$$

Moreover, the temperature difference ΔT is given by $\Delta T = T_{q_2} - T_{q_1}$ if $T_{q_1} < T_{q_2}$. As a consequence, the dimensionless parameter R_T can only take the values 0 or 1. More precisely, the temperature difference ratio R_T is equal to 1 for asymmetric heating i.e. $T_{q_1} < T_{q_2}$, while $R_T = 0$ for symmetric heating i.e. $T_{q_1} = T_{q_2}$, respectively. Equation 17 implies that A can be either positive or negative. If $A < 0$, then U_0^i, Re and Λ are negative, i.e. the flow is downward. On the other hand, if $A > 0$, the flow is upward, so that U_0^i, Re, and Λ are positive. Using Eqs. 25 and 26, Eqs. 20-24 becomes

Region-I

$$\frac{d^4u_1}{dy^4} - \sigma^2\frac{d^2u_1}{dy^2} = \Lambda Br\left(\left(\frac{du_1}{dy}\right)^2 + \sigma^2 u_1^2\right) \tag{27}$$

Region-II

$$\frac{d^4u_2}{dy^4} = \Lambda Br\, bh^4 knm\left(\frac{du_2}{dy}\right)^2 \tag{28}$$

The boundary and interface conditions becomes

$$u_1\left(-1/4\right) = u_2\left(1/4\right) = 0,$$

$$u_1(0) = mh^2u_2(0), \qquad \frac{du_1(0)}{dy} = h\frac{du_2(0)}{dy},$$

$$\left(\frac{d^2u_1}{dy^2} - \sigma^2u_1\right) = \frac{1}{nb}\frac{d^2u_2}{dy^2} + \frac{48(1-nb)}{nb} \text{ at } y = 0$$

$$\left(\frac{d^3u_1}{dy^3} - \sigma^2\frac{du_1}{dy}\right) = \frac{1}{nbkh}\frac{d^3u_2}{dy^3} \qquad \text{at } y = 0$$

$$\left(\frac{d^2u_1}{dy^2}+\frac{\sigma^2}{Bi_1}\frac{du_1}{dy}-\frac{1}{Bi_1}\frac{d^3u_1}{dy^3}\right)_{y=-1/4}=-48+\frac{R_T}{2}\Lambda s\left(1+\frac{4}{Bi_1}\right),$$

$$\left(\frac{d^2u_2}{dy^2}+\frac{1}{Bi_2}\frac{d^3u_2}{dy^3}\right)_{y=1/4}=-48-\frac{R_T}{2}sbn\Lambda\left(1+\frac{4}{Bi_2}\right) \quad (29)$$

Basic Idea of Differential transformation method (DTM)

Suppose $u(y)$ is analytic in a domain *D*, then it will be differentiated continuously with respect to y in the domain of interest. The differential transform of function $u(y)$ is defined as

$$U(k)=\frac{1}{k!}\left[\frac{d^k u(y)}{dy^k}\right]_{y=0} \quad (30)$$

where $u(y)$ is the original function and $U(k)$ is the transformed function which is called the T-function.

The differential inverse transform of $U(k)$ is defined as follows:

$$u(y)=\sum_{k=0}^{\infty}U(k)y^k \quad (31)$$

In real applications, the function $u(y)$ by a finite series of Eq. 31 can be written as

$$u(y)=\sum_{k=0}^{n}U(k)y^k \quad (32)$$

and Eq. 31 implies that $u(y)=\sum_{k=n+1}^{\infty}U(k)y^k$ and is neglected as it is small. Usually, the values of *n* are decided by a convergence of the series coefficients.

The fundamental mathematical operations performed by differential transform method are listed in Table 1.

Table 1. The Operations for the One-Dimensional Differential Transform Method.

Original function	Transformed function
$y(x)=g(x)\pm h(x)$	$Y(k)=G(k)\pm H(k)$
$y(x)=\alpha g(x)$	$Y(k)=\alpha G(k)$
$y(x)=\frac{dg(x)}{dx}$	$Y(k)=(k+1)G(k+1)$
$y(x)=\frac{d^2g(x)}{dx^2}$	$Y(k)=(k+1)(k+2)G(k+2)$
$y(x)=g(x)h(x)$	$Y(k)=\sum_{l=0}^{k}G(l)H(k-l)$
$y(x)=x^m$	$Y(k)=\delta(k-m)=\begin{cases}1, \text{ if } k=m\\0, \text{ if } k\neq m\end{cases}$

Solutions

Case of Negligible Viscous Dissipation $(Br=0)$

The solution of Eqs. 27 and 28 using boundary and interface conditions defined as in Eq. 29 in the absence of viscous dissipation term $(Br=0)$ is given by

Region-I

$$u_1=c_1+c_2y+c_3\cosh(\sigma y)+c_4\sinh(\sigma y) \quad (33)$$

Region-II

$$u_2=c_5+c_6y+c_7y^2+c_8y^3 \quad (34)$$

Using Eq. 29 in Eqs. 5 and 6, the energy balance equations becomes

Region-I

$$\theta_1=-\frac{1}{\Lambda}\left(48+\frac{d^2u_1}{dy^2}-\sigma^2u_1\right) \quad (35)$$

Region-II

$$\theta_2=-\frac{1}{\Lambda bn}\left(48+\frac{d^2u_2}{dy^2}\right) \quad (36)$$

Using the expressions obtained in Eqs. 33 and 34 the energy balance Eqs. 35 and 36 becomes

Region-I

$$\theta_1=-\frac{1}{\Lambda}\left(48-\sigma^2\left(c_1+c_2y\right)\right) \quad (37)$$

Region-II

$$\theta_2=-\frac{1}{\Lambda bn}\left(48+2c_7+6c_8y\right) \quad (38)$$

Case of Negligible Buoyancy Force $(\Lambda=0)$

The solution of Eqs. 27 and 28 can be obtained when buoyancy forces are negligible ($\Lambda=0$) and viscous dissipation is dominating ($Br\neq 0$), so that purely forced convection occurs. For this case,solutions of Eqs. 27 and 28, using the boundary and interface conditions given by Eq. 29, the velocities are given by

Region-I

$$u_1=d_1+d_2y+d_3\cosh(\sigma y)+d_4\sinh(\sigma y) \quad (39)$$

Region-II

$$u_2=d_5+d_6y+d_7y^2+d_8y^3 \quad (40)$$

The energy balance Eqs. 18 and 19 in non-dimensional form can also be written as

Region-I

$$\frac{d^2\theta_1}{dy^2}=-Br\left(\left(\frac{du_1}{dy}\right)^2+\sigma^2u_1^2\right) \quad (41)$$

Region-II

$$\frac{d^2\theta_2}{dy^2}=-Br\,kmh^4\left(\frac{du_2}{dy}\right)^2 \quad (42)$$

The boundary and interface conditions for temperature are

$$\left.\frac{d\theta_1}{dy}\right|_{y=-1/4}-Bi_1\theta_1(-1/4)=\frac{Bi_1R_Ts}{2}\left(1+\frac{4}{Bi_1}\right)$$

$$\left.\frac{d\theta_2}{dy}\right|_{y=1/4}+Bi_2\theta_2(1/4)=\frac{Bi_2R_Ts}{2}\left(1+\frac{4}{Bi_2}\right)$$

$$\theta_1(0)=\theta_2(0);\quad \frac{d\theta_1(0)}{dy}=\frac{1}{kh}\frac{d\theta_2(0)}{dy} \quad (43)$$

Using Eqs. 39 and 40, solving Eqs. 41 and 42 we obtain

Region-I

$$\theta_1=-Br\begin{pmatrix}G_1\cosh(2\sigma y)+G_2\sinh 2\sigma y\\+G_3\cosh(\sigma y)+G_4\sinh(\sigma y)\\+G_5y\cosh(\sigma y)+G_6y\sinh(\sigma y)\\+G_7y^4+G_8y^3+G_9y^2\end{pmatrix}+F_1y+F_2 \quad (44)$$

Region-II

$$\theta_2=G_{10}y^2+G_{11}y^3+G_{12}y^4+G_{13}y^5+G_{14}y^6+F_3y+F_4 \quad (45)$$

Combined Effects of Buoyancy Forces and Viscous Dissipation

We solve Eqs. 27 and 28 using the perturbation method (PM) with a dimensionless parameter $|\varepsilon|$ (<<1) defined as

$$\varepsilon = \Lambda Br \tag{46}$$

and does not depend on the reference temperature difference ΔT. To this end the solutions are assumed in the form

$$u(y) = u_0(y) + \varepsilon u_1(y) + \varepsilon^2 u_2(y) + ... = \sum_{n=0}^{\infty} \varepsilon^n u_n(y) \tag{47}$$

Substituting Eq.47 in Eqs. 27 and 28 and equating the coefficients of like powers of ε to zero, we obtain the zero and first order equations as follows:

Region-I

Zeroth-order equations

$$\frac{d^4u_{10}}{dy^4} - \sigma^2 \frac{d^2u_{10}}{dy^2} = 0 \tag{48}$$

First-order equations

$$\frac{d^4u_{11}}{dy^4} - \sigma^2 \frac{d^2u_{11}}{dy^2} = \left(\frac{du_{10}}{dy}\right)^2 + \sigma^2 u_{10}^2 \tag{49}$$

Region-II

Zeroth-order equations

$$\frac{d^4u_{20}}{dy^4} = 0 \tag{50}$$

First-order equations

$$\frac{d^4u_{21}}{dy^4} = mnbkh^4 \left(\frac{du_{20}}{dy}\right)^2 \tag{51}$$

The corresponding boundary and interface conditions given by Eq. 29 for the zeroth and first order reduces to

Zeroth-order

$$u_{10}(-1/4) = u_{20}(1/4) = 0,$$

$$u_{10}(0) = mh^2 u_{20}(0), \quad \frac{du_{10}(0)}{dy} = h\frac{du_{20}(0)}{dy}$$

$$\left(\frac{d^2u_{10}}{dy^2} - \sigma^2 u_{10}\right) = \frac{1}{nb}\frac{d^2u_{20}}{dy^2} + \frac{48(1-nb)}{nb} \quad \text{at} \quad y = 0$$

$$\left(\frac{d^3u_{10}}{dy^3} - \sigma^2 \frac{du_{10}}{dy}\right) = \frac{1}{nbkh}\frac{d^3u_{20}}{dy^3} \quad \text{at} \quad y = 0$$

$$\left(\frac{d^2u_{10}}{dy^2} + \frac{\sigma^2}{Bi_1}\frac{du_{10}}{dy} - \frac{1}{Bi_1}\frac{d^3u_{10}}{dy^3}\right)_{y=-1/4} = -48 + \frac{R_T}{2}\Lambda s\left(1 + \frac{4}{Bi_1}\right)$$

$$\left(\frac{d^2u_{20}}{dy^2} + \frac{1}{Bi_2}\frac{d^3u_{20}}{dy^3}\right)_{y=1/4} = -48 - \frac{R_T}{2}\Lambda sbn\left(1 + \frac{4}{Bi_2}\right) \tag{52}$$

First-order

$$u_{11}(-1/4) = u_{21}(1/4) = 0$$

$$u_{11}(0) = mh^2 u_{21}(0); \quad \frac{du_{11}(0)}{dy} = h\frac{du_{21}(0)}{dy}$$

$$\left(\frac{d^2u_{11}}{dy^2} - \sigma^2 u_{11}\right) = \frac{1}{nb}\left(\frac{d^2u_{21}}{dy^2}\right) \text{ at} \quad y = 0$$

$$\left(\frac{d^3u_{11}}{dy^3} - \sigma^2 \frac{du_{11}}{dy}\right) = \frac{1}{nbkh}\frac{d^3u_{21}}{dy^3} \quad \text{at} \quad y = 0,$$

$$\left(\frac{d^2u_{11}}{dy^2} + \frac{\sigma^2}{Bi_1}\frac{du_{11}}{dy} - \frac{1}{Bi_1}\frac{d^3u_{11}}{dy^3}\right)_{y=-1/4} = 0;$$

$$\left(\frac{d^2u_{21}}{dy^2} + \frac{1}{Bi_2}\frac{d^3u_{21}}{dy^3}\right)_{y=1/4} = 0 \tag{53}$$

Solutions of zeroth-order Eqs.48 and 50 using boundary and interface conditions as in Eq.52 are

$$u_{10} = H_1 + H_2 y + H_3 \cosh(\sigma y) + H_4 \sinh(\sigma y) \tag{54}$$

$$u_{20} = H_5 + H_6 y + H_7 y^2 + H_8 y^3 \tag{55}$$

Solutions of first-order Eqs.49 and 51 using boundary and interface conditions as in Eq. 53 are

$$\begin{aligned} u_{11} = {} & H_9 + H_{10}y + H_{11}\cosh(\sigma y) + H_{12}\sinh(\sigma y) + k_{10}\cosh(2\sigma y) \\ & + k_{11}\sinh(2\sigma y) + k_{12}y\sinh(2\sigma y) + k_{13}y\cosh(\sigma y) \\ & + k_{14}y^2\cosh(\sigma y) + k_{15}y^2\sinh(\sigma y) + k_{16}y^4 + k_{17}y^3 + k_{18}y^2 \end{aligned} \tag{56}$$

$$u_{21} = M_5 y^8 + M_6 y^7 + M_7 y^6 + M_8 y^5 + M_9 y^4 + \frac{M_1}{6}y^3 + \frac{M_2}{2}y^2 + M_3 y + M_4 \tag{57}$$

Using velocities given by Eqs. 54-57, the expressions for energy balance Eqs. 35 and 36 becomes

Region-I

$$\theta_1 = -\frac{1}{\Lambda}\begin{pmatrix} 48 + \varepsilon\left(4\sigma^2 k_{10}\cosh(2\sigma y) + 4\sigma^2 k_{11}\sinh(2\sigma y)\right. \\ + 2\sigma k_{12}\cosh(\sigma y) + 2\sigma k_{13}\sinh(\sigma y) \\ + k_{14}\left(4\sigma y\sinh(\sigma y) + 2\cosh(\sigma y)\right) + \\ k_{15}\left(4\sigma y\cosh(\sigma y) + 2\sinh(\sigma y)\right) \\ + 12k_{16}y^2 + 6k_{17}y + 2k_{18} - \sigma^2\left(H_9 + H_{10}y\right. \\ + k_{10}\cosh(2\sigma y) + k_{11}\sinh(2\sigma y) \\ \left.\left. + k_{16}y^4 + k_{17}y^3 + k_{18}y^2\right)\right) - \sigma^2\left(H_1 + H_2 y\right) \end{pmatrix} \tag{58}$$

Region-II

$$\begin{aligned} \theta_2 = {} & -\frac{1}{\Lambda bn}\left(48 + 2H_7 + 6H_8 y + \varepsilon\left(56M_5 y^6 + 42M_6 y^5\right.\right. \\ & \left.\left. + 30M_7 y^4 + 20M_8 y^3 + 2M_9 y^2 + M_1 y + M_2\right)\right) \end{aligned} \tag{59}$$

Solution with Differential Transform method

Differential Transformation Method has been applied for solving Eqs. 27 and 28. Taking the differential transformation of Eqs.27 and 28 with respect to k, and following the process as given in Table 1 yields:

$$\begin{aligned} U(r+4) = {} & \frac{1}{(r+1)(r+2)(r+3)(r+4)}\left(\sigma^2(r+1)(r+2)U(r+2)\right. \\ & \left. + \Lambda Br\sum_{s=0}^{r}(r-s+1)(s+1)U(r-s+1)U(s+1)\right) \end{aligned} \tag{60}$$

$$V(r+4) = \frac{1}{(r+1)(r+2)(r+3)(r+4)}\left(\Lambda Br A_1\sum_{s=0}^{r}(r-s+1)(s+1)\,V(r-s+1)\,V(s+1)\right) \tag{61}$$

The differential transform of the initial conditions are as follows

$$U(0) = c_1;\ U(1) = c_2;\ U(2) = \frac{c_3}{2!};\ U(3) = \frac{c_4}{3!};\ V(0) = \frac{c_1}{mh^2},$$

$$V(1)=\frac{c_2}{h};\ V(2)=\frac{\left(c_3-\sigma^2 c_1\right)nb+48(nb-1)}{2};$$
$$U(3)=\frac{\left(c_4-\sigma^2 c_2\right)nbkh}{6} \qquad (62)$$

where $U(r)$ and $V(r)$ are the transformed versions of $u_1(y)$ and $u_2(y)$ respectively.

Using the conditions as given in Eq.62, one can evaluate the unknowns c_1, c_2, c_3, and c_4. By using the DTM and the transformed boundary conditions, above equations that finally leads to the solution of a system of algebraic equations.

A Nusselt number can be defined at each boundary, as follows

$$Nu_1=\frac{(1+h)}{R_T\left[\theta_2(1/4)-\theta_1(-1/4)\right]+(1-R_T)}\frac{d\theta_1}{dy}\bigg|_{y=-1/4}$$
$$Nu_2=\frac{(1+1/h)}{R_T\left[\theta_2(1/4)-\theta_1(-1/4)\right]+(1-R_T)}\frac{d\theta_2}{dy}\bigg|_{y=1/4} \qquad (63)$$

Result and discussion

Mixed convection flow and heat transfer in a vertical channel containing fluid and porous layers is investigated with boundary conditions of third kind. The flow is modeled with Darcy-Lapwood-Brinkman equation. The viscous and Darcy dissipation terms are included in the energy equation. The analytical solutions are found using regular Perturbation method with the product of mixed convection parameter $\Lambda(Gr/\mathrm{Re})$ and Brinkman number Br as perturbation parameter. Since the analytical solutions are valid only for small values of the perturbation parameter $\varepsilon(<1)$, the governing equations are solved using Differential Transform Method which is a semi analytical method valid for all values of ε.

The flow field in the case of asymmetric heating $(R_T=1)$ and symmetric heating $(R_T=0)$ for equal and unequal Biot numbers are obtained and shown graphically in Figures 2-12 in the absence of viscous dissipation. The velocity is evaluated and is shown in Fig. 2 for different values of porous parameter σ for equal Biot numbers. It is seen that velocity profiles for $\Lambda=400$ shows a flow reversal near the cold wall at $y=-1/4$. It is also observed from Fig. 2 that as the porous parameter σ increases velocity decreases for all values of Λ.

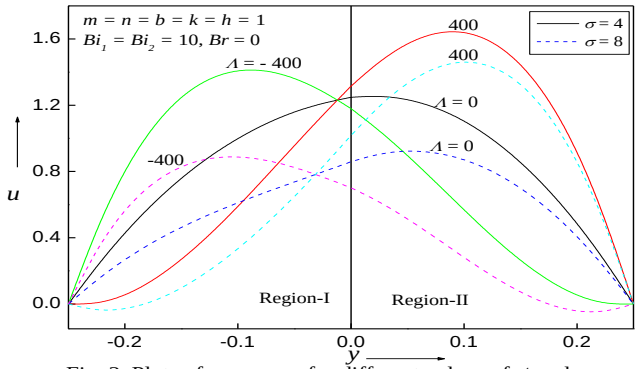

Fig. 2. Plots of u versus y for different values of Λ and σ.

In the absence of mixed convection parameter Λ the non-dimensional temperature field θ is evaluated for different values of Brinkman number Br and are shown in Figs.3a,b for equal and unequal Biot numbers respectively. It is seen from Figs. 3a,b that in the absence of mixed convection parameter Λ and viscous dissipation $(Br=0)$, the temperature field is linear indicating that the heat transfer is purely by conduction. Although the conduction region holds for $Br=0$, the temperature is almost linear in the middle of the channel for $Br\neq 0$ also indicating that the convection dominates in the boundary region. As Brinkman number Br increases the temperature field increases for both equal and unequal Biot numbers. Further these two figures also reveal that for any value of Brinkman number the temperature decreases as the porous parameter σ increases for both equal and unequal Biot numbers. The nature of profiles in the absence of viscous dissipation (Fig. 2) and mixed convection parameter Λ (Figs. 3a, b) are the similar result obtained by Umavathi and Santhosh [30, 31] for one fluid model.

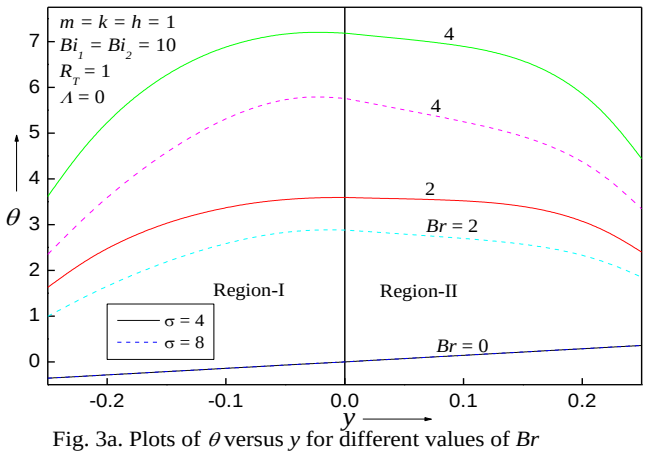

Fig. 3a. Plots of θ versus y for different values of Br

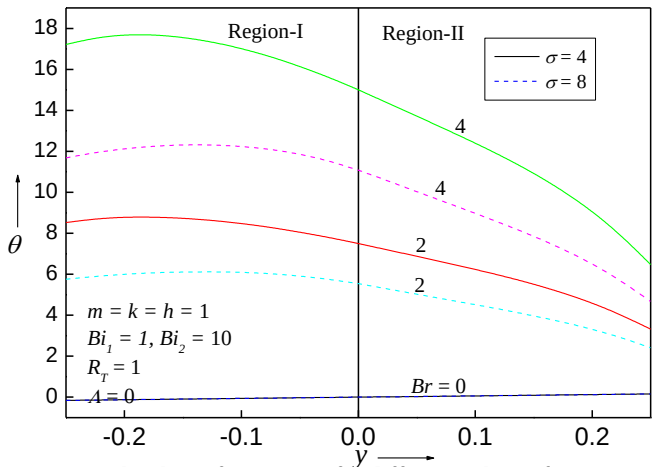

Fig. 3b. Plots of θ versus y for different values of Br

The effect of porous parameter σ on the flow for upward $(\Lambda>0)$ and for downward $(\Lambda<0)$ flow for equal Biot numbers is shown in Figs. 4a, b. As the porous parameter σ increases the fluid velocity decreases both in the porous region and also in clear viscous fluid region. This is because of the fact that for large porous parameter σ, the frictional drag resistance against the convection is very large and as a result the velocity is very small in the porous region. The velocity also decreases in clear viscous fluid region as σ increases, which is due to the dragging effect from the porous region to clear viscous region at the interface. There is no much effect of porous parameter σ on the temperature as seen in Fig.4b. The effect of porous parameter

σ on the flow was the similar result obtained by Umavathi and Santhosh [30, 31] for one fluid model.

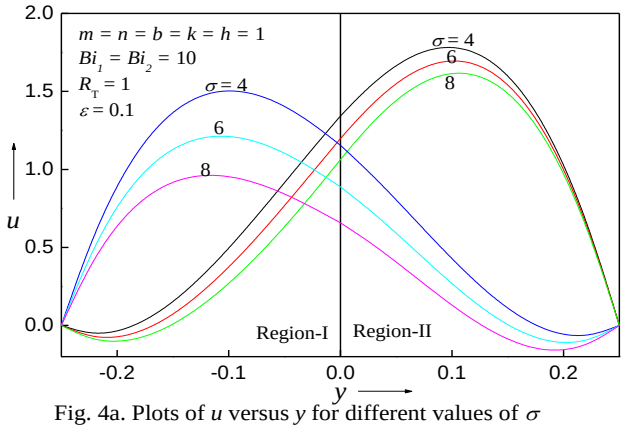

Fig. 4a. Plots of u versus y for different values of σ

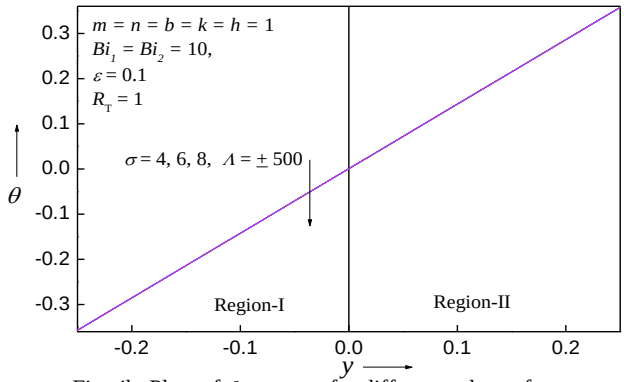

Fig. 4b. Plots of θ versus y for different values of σ

Figures 5a and 5b shows the variation of non-dimensional velocity u and temperature θ profiles for $\Lambda = \pm 500$, $\sigma = 4$ and for different values of ε for equal Biot numbers. For upward flow $(\varepsilon > 0)$ the velocity and temperature fields are increasing functions of ε and for downward flow $(\varepsilon < 0)$ velocity field is a decreasing function of ε, where as temperature is an increasing functions of ε. The effect of ε on velocity field is stronger while that on the temperature field is weaker. One can also reveal from the Fig. 5a that flow reversal occurs at the left wall for upward flow and at the right wall for downward flow. This is because the increase in perturbation parameter ε implies the enhancement of viscous dissipation which results in higher values of temperature which in turn enhances the buoyancy force. Therefore increase in the buoyancy force increases the fluid flow for $\varepsilon > 0$ and decreases the fluid flow for $\varepsilon < 0$. Figures 5a and 5b also reveal that the PM and DTM solutions are close for $\varepsilon = 0$ and differ substantially as ε increases. The effect of Λ and ε show the similar result observed by Prathap Kumar et al. [17] for isothermal boundary conditions and also by Umavathi and Santhosh [30, 31] for one fluid model for boundary conditions of third kind.

The effect of viscosity ratio parameter m on the flow for equal Biot numbers is depicted graphically in Figs. 6a and 6b for $\Lambda = 500$. As the viscosity ratio m increases the velocity increases in the porous region and decreases in the viscous region. This nature can be interpreted as follows. The viscosity ratio m is taken as the ratio of viscosity of the porous region to the viscosity of the clear fluid region. Increase in the value of m for values of $m > 1$ implies the viscosity of porous medium is less than the viscosity of clear fluid region and hence the velocity decreases in the clear fluid region as m increases. Further the magnitude of velocity in Region-II is less than the magnitude of velocity in Region-I. The jump at the interface is due to the interface condition imposed at the interface. Further one can also observe that as the porous parameter σ increases the velocity decreases in both the regions. However its effect is not significant on temperature field.

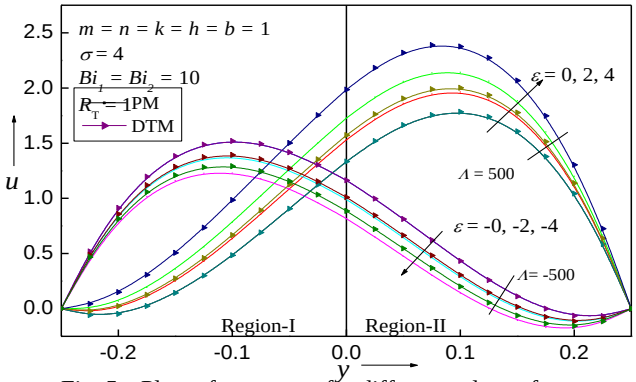

Fig. 5a. Plots of u versus y for different values of ε

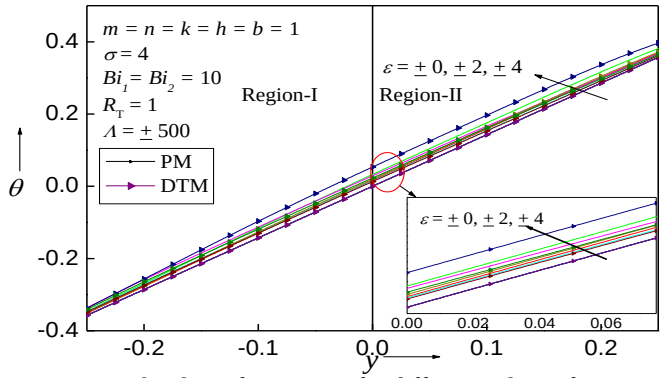

Fig. 5b. Plots of θ versus y for different values of ε

The effect of width ratio parameter h on the velocity and temperature fields is shown in Figs. 7a and 7b respectively. As the parameter h increases both the velocity and temperature fields decreases. The width ratio h is taken as the ratio of clear fluid layer to porous fluid layer. As the parameter h increases implies that increase in the width of the clear fluid layer compared to that of porous fluid layer, the weaker the flow field. It can also be seen from the Figs. 7a and 7b that the magnitude of velocity and temperature is less in the porous fluid layer compared to the viscous fluid layer. Further one can also explore from these figures that as the porous parameter increases the velocity decreases both in the porous and viscous fluid layer. However the effect of σ on temperature is not significant.

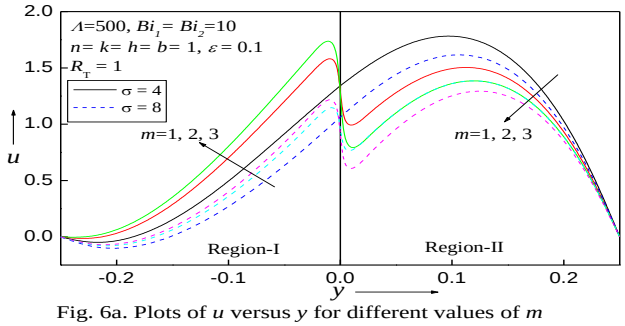

Fig. 6a. Plots of u versus y for different values of m

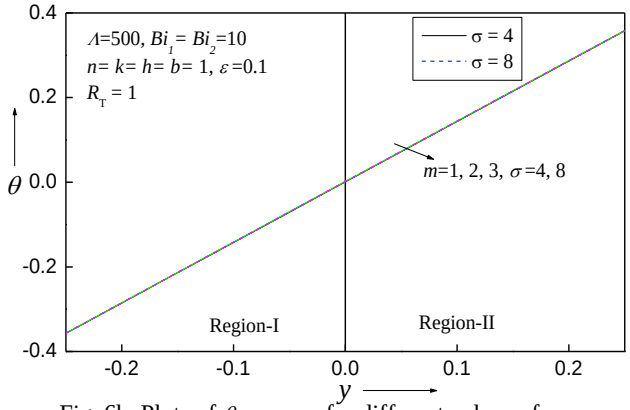

Fig. 6b. Plots of θ versus y for different values of m

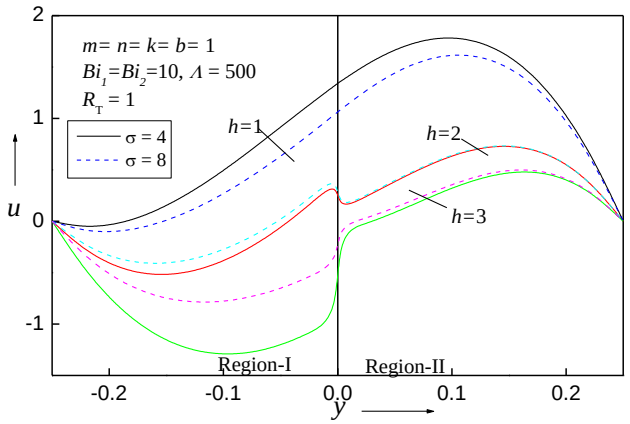

Fig. 7a. Plots of u versus y for different values of h

The effect of conductivity ratio $k\left(k_1/k_2\right)$ on the velocity and temperature fields is shown in the Figs. 8a and 8b respectively for equal Biot numbers. As the conductivity ratio k increases both the velocity and temperature fields decreases. That is to say that larger the thermal conductivity of the clear fluid layer compared to the porous fluid layer, the smaller the velocity and temperature field. Figures 8a and 8b also reflects that as the porous parameter σ increases velocity decreases in both the regions and is invariant on temperature field. The effect of m, h and k on the flow was the similar result obtained by Prathap Kumar et al. [17] for isothermal boundary conditions.

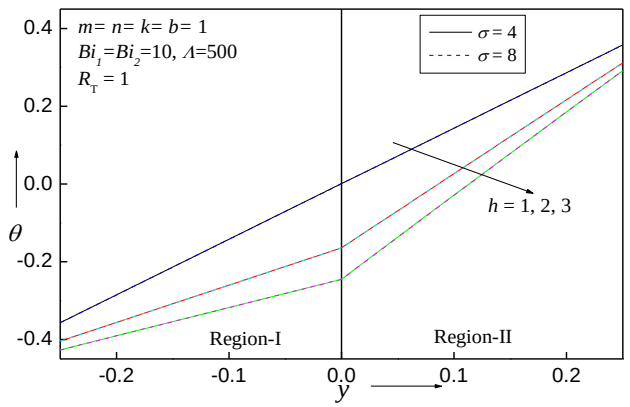

Fig. 7b. Plots of θ versus y for different values of h

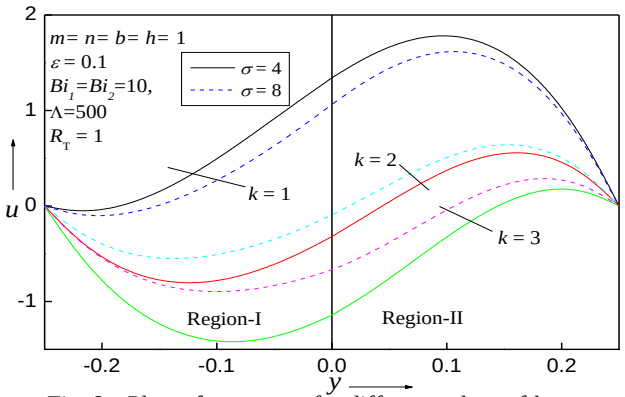

Fig. 8a. Plots of u versus y for different values of k

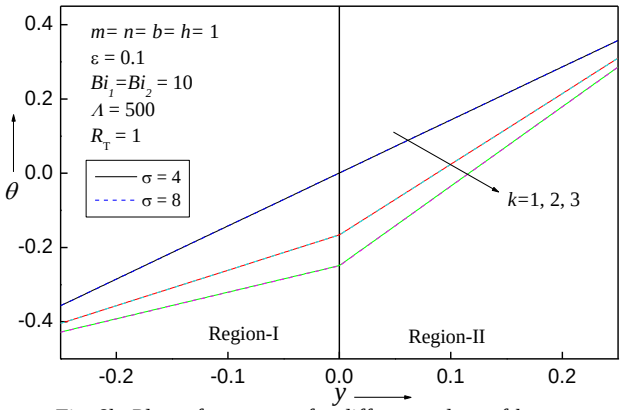

Fig. 8b. Plots of θ versus y for different values of k

Figures 9a and 9b are the dimensionless velocity u and temperature θ for different values of ε and Λ considering different values for Biot numbers at the left and right walls. It is noticed that there is no flow reversal for large values of mixed convection parameter Λ for unequal Biot numbers when compared with equal Biot numbers for both upward $(\varepsilon > 0)$ and for downward $(\varepsilon < 0)$ flow. Further it is also observed from Fig. 9b that temperature increases more at the cold wall when compared with the hot wall. That is to say that temperature increases more at the wall which has smaller external convection coefficient. Comparing the flow nature for equal Biot numbers (Figs. 5a,b) and for unequal Biot numbers (Figs. 9a,b) reveals that effect of Λ on u and θ becomes stronger if either Bi_1 or Bi_2 becomes stronger. The effect of porous parameter σ on u and θ for unequal Biot numbers is depicted in Figs. 10a,b. Here also as the porous parameter σ increases velocity decreases in both the regions for both buoyancy assisting $(\Lambda > 0)$ and buoyancy opposing $(\Lambda < 0)$ flow and temperature remains invariant. The effect of ε, Λ and σ for unequal Biot numbers on the velocity and temperature field was the similar result observed by Umavathi and Santhosh [30] for one fluid model.

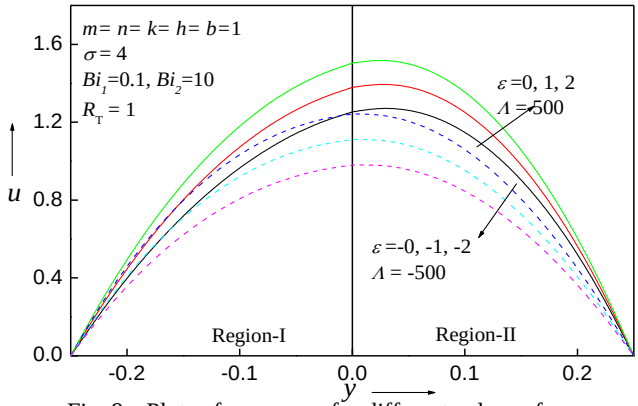

Fig. 9a. Plots of u versus y for different values of ε

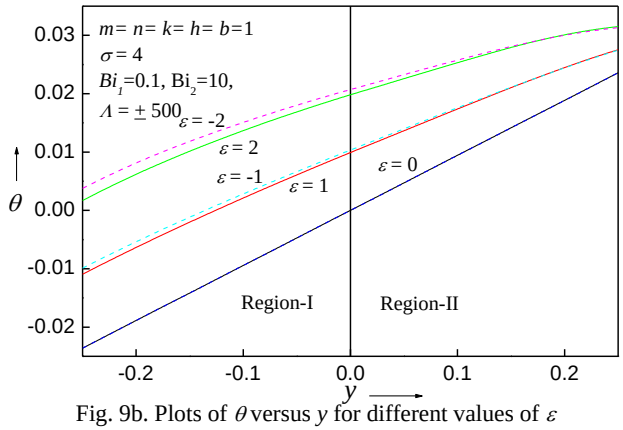

Fig. 9b. Plots of θ versus y for different values of ε

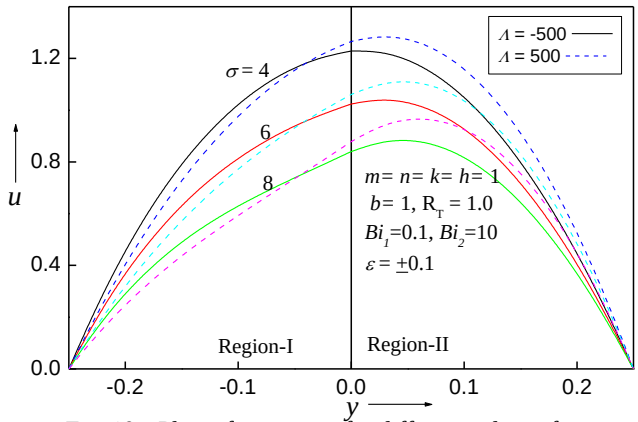

Fig. 10a. Plots of u versus y for different values of σ

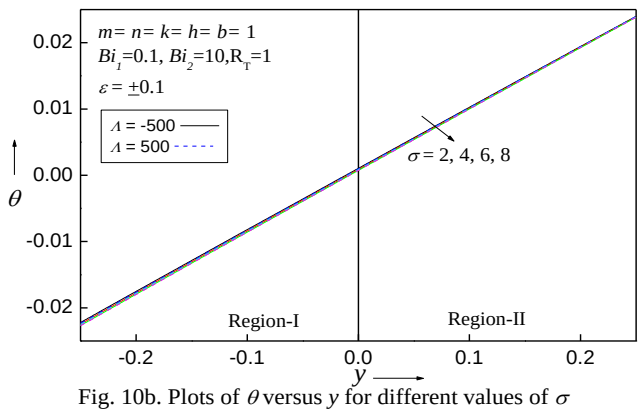

Fig. 10b. Plots of θ versus y for different values of σ

Figures 11a,b and 12a,b shows the velocity and $\Lambda\theta$ for symmetric wall heating condition for equal and unequal Biot numbers. It is observed from these figures that both u and $\Lambda\theta$ are increasing functions of ε. These Figures also reveal that the temperature profiles are symmetric for equal Biot numbers and is more significant in the case of upward flow than in the case of downward flow. Further one can also come to the conclusion that the effect of Λ on u and θ become stronger if either Bi_1 or Bi_2 becomes smaller for symmetric heating also (similar nature was also observed for asymmetric heating). The effect of Bi_1 and Bi_2 for asymmetric and symmetric heating on the flow show the similar nature obtained by Umavathi and Santhosh [30] for one fluid model.

Figures 9a,b, 11a,b and 12a,b suggest that the solutions obtained by PM and DTM agree very well for small values of ε and the difference becomes very large as ε increases for both assisting and opposing flow.

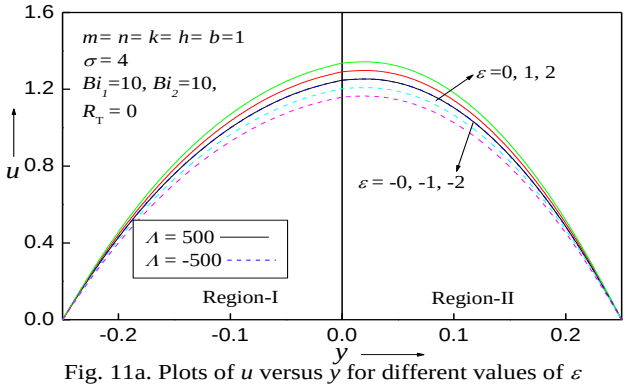

Fig. 11a. Plots of u versus y for different values of ε

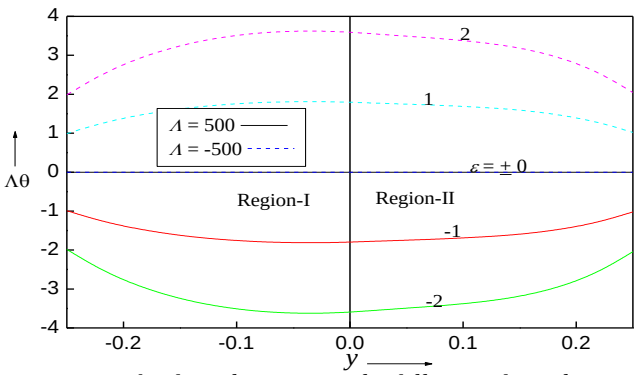

Fig. 11b. Plots of $\Lambda\theta$ versus y for different values of ε

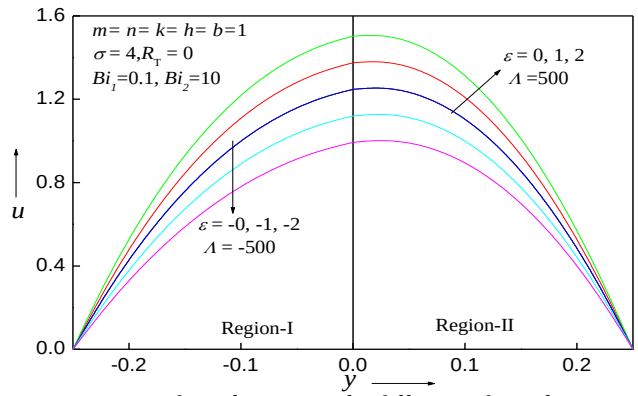

Fig. 12a. Plots of u versus y for different values of ε

The rate of heat transfer at both the walls for variation of $|\varepsilon|$ is shown in Fig.13. The Nusselt numbers at the cold wall is a decreasing function of mixed convection parameter Λ for upward flow and increasing function of Λ for downward flow. The rate of heat transfer is more for smaller values of Λ at the left wall. The Nusselt number is an increasing function of mixed convection parameter Λ for downward flow at the hot wall and decreasing function of Λ for upward flow. The flow nature of Nusselt number on $|\varepsilon|$ is the similar result obtained by Umavathi and Santhosh [30,31] for one fluid model.

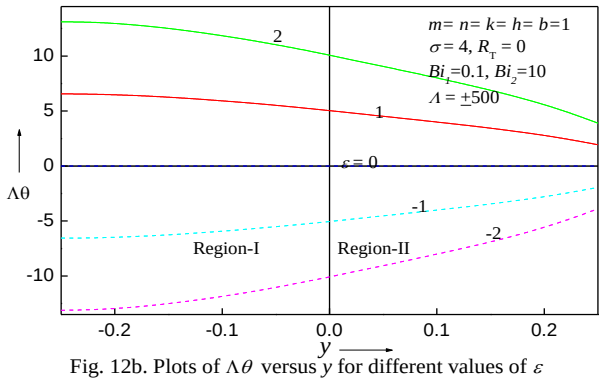

Fig. 12b. Plots of $\Lambda\theta$ versus y for different values of ε

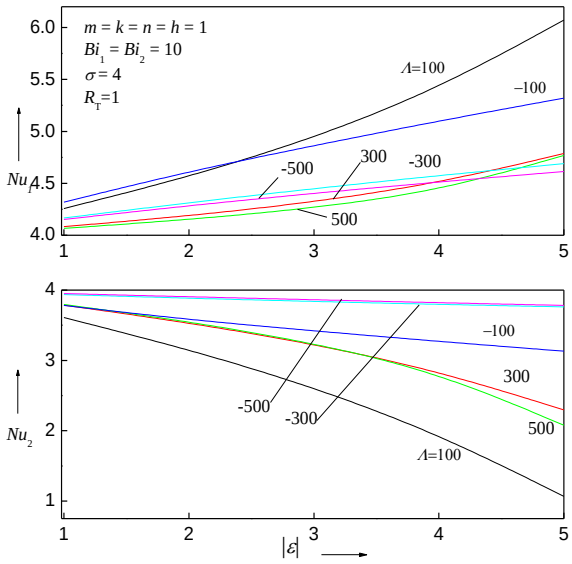

Fig. 13. Plots of Nu_1 and Nu_2 versus $|\varepsilon|$ for different values of Λ

Tables 2-4 are the velocity and temperature solutions obtained by PM and DTM for symmetric and asymmetric wall heating conditions varying the perturbation parameter ε for equal and unequal Biot numbers. In Table 2, it is seen that in the absence of perturbation parameter, the PM and DTM solutions are equal for both the velocity and temperature fields. When the perturbation parameter ε is increased $(\varepsilon = 2)$, it is seen that the PM and DTM solutions do not agree. Similar nature is also observed in Table3 and 4 for PM and DTM solutions. Table 2 and 3 are the solutions of velocity and temperature for asymmetric wall heating conditions for equal and uneqal Biot numbers respectively. Table 2 and 3 also reveals that the percentage of error is large at the interface for velocity when compared with the error at the boundaries. Further the percentage of error between PM and DTM is large for unequal Biot numbers when compared with eqal Biot numbers. Table 4 display the solutions of symmetric wall heating conditions for equal Biot numbers. The percentage of error is less for symmetric wall heating conditions for equal Biot numbers when compared with asymmetric wall heat conditions.

Table 2. Values of Velocity and Temperature for $\Lambda = 500$ and $R_T = 1, \sigma = 4$

y	$\varepsilon = 0$, $Bi_1 = Bi_2 = 10$			$\varepsilon = 2$, $Bi_1 = Bi_2 = 10$		
	PM	DTM	% Error	PM	DTM	% Error
	Velocity					
-0.25	0.00000	0.00000	0.00	0.00000	0.00000	0.00
-0.15	0.14181	0.14181	0.00	0.25104	0.27456	2.35
-0.05	0.90598	0.90598	0.00	1.08579	1.12404	3.82
0.00	1.33271	1.33271	0.00	1.53026	1.57208	4.18
0.05	1.66331	1.66331	0.00	1.86211	1.90410	4.20
0.15	1.60737	1.60737	0.00	1.74692	1.77639	2.95
0.25	0.00000	0.00000	0.00	0.00000	0.00000	0.00
	Temperature					
-0.25	-0.35714	-0.35714	0.00	-0.35147	-0.35019	0.13
-0.15	-0.21429	-0.21429	0.00	-0.20306	-0.20052	0.25
-0.05	-0.07143	-0.07143	0.00	-0.05600	-0.05272	0.33
0.00	0.00000	0.00000	0.00	0.01633	0.01973	0.34
0.05	0.07143	0.07143	0.00	0.08793	0.09135	0.34
0.15	0.21429	0.21429	0.00	0.23058	0.23404	0.35
0.25	0.35714	0.35714	0.00	0.36922	0.37171	0.25

Table 3. Values of Velocity and Temperature for $\Lambda = 500$ and $R_T = 1, \sigma = 4$

y	$\varepsilon = 0$, $Bi_1 = 1, Bi_2 = 10$			$\varepsilon = 2$, $Bi_1 = 1, Bi_2 = 10$		
	PM	DTM	% Error	PM	DTM	% Error
	Velocity					
-0.25	0.00000	0.00000	0.00	0.00000	0.00000	0.00
-0.15	0.49088	0.49088	0.00	0.55630	0.56788	1.16
-0.05	1.04996	1.04996	0.00	1.14759	1.16459	1.70
0.00	1.28498	1.28498	0.00	1.38810	1.40592	1.78
0.05	1.42424	1.42424	0.00	1.52459	1.54182	1.72
0.15	1.18649	1.18649	0.00	1.25303	1.26431	1.13
0.25	0.00000	0.00000	0.00	0.00000	0.00000	0.00
	Temperature					
-0.25	-0.15625	-0.15625	0.00	-0.14814	-0.14660	0.15
-0.15	-0.09375	-0.09375	0.00	-0.08504	-0.08345	0.16
-0.05	-0.03125	-0.03125	0.00	-0.02264	-0.02113	0.15
0.00	0.00000	0.00000	0.00	0.00823	0.00965	0.14
0.05	0.03125	0.03125	0.00	0.03897	0.04028	0.13
0.15	0.09375	0.09375	0.00	0.10038	0.10146	0.11
0.25	0.15625	0.15625	0.00	0.16054	0.16120	0.07

Table 4 Values of Velocity and Temperature for $R_T = 0, \sigma = 4$

y	$\varepsilon = 0$, $Bi_1 = Bi_2 = 10$			$\varepsilon = 2$, $Bi_1 = Bi_2 = 10$		
	PM	DTM	% Error	PM	DTM	% Error
	Velocity					
-0.25	0.00000	0.00000	0.00	0.00000	0.00000	0.00
-0.15	0.76238	0.76238	0.00	0.81554	0.82474	0.92
-0.05	1.16194	1.16194	0.00	1.24466	1.25897	1.43
0.00	1.24786	1.24786	0.00	1.33665	1.35201	1.54
0.05	1.23829	1.23829	0.00	1.32593	1.34108	1.52
0.15	0.85915	0.85915	0.00	0.91858	0.92884	1.03
0.25	0.00000	0.00000	0.00	0.00000	0.00000	0.00
	Temperature					
-0.25	0.00000	0.00000	0.00	0.00397	0.00465	0.07
-0.15	0.00000	0.00000	0.00	0.00650	0.00762	0.11
-0.05	0.00000	0.00000	0.00	0.00725	0.00850	0.13
0.00	0.00000	0.00000	0.00	0.00718	0.00843	0.13
0.05	0.00000	0.00000	0.00	0.00699	0.00819	0.12
0.15	0.00000	0.00000	0.00	0.00638	0.00748	0.11
0.25	0.00000	0.00000	0.00	0.00408	0.00478	0.07

Conclusions

The analytical (PM) and semi-analytical (DTM) solutions were found for the problem of steady laminar mixed convective flow in a vertical channel filled with porous and fluid layers using boundary conditions of third kind. The following conclusions were drawn.

1. The flow at each position was an increasing function of ε for upward flow and decreasing function of ε for downward flow.
2. The porous parameter suppresses the flow for symmetric and asymmetric wall heating conditions for all the governing parameters.
3. Flow reversal was observed for asymmetric wall heating for equal Biot numbers and there is no flow reversal for unequal Biot numbers.
4. The viscosity ratio increases the flow in porous region and decreases in viscous region for equal Biot numbers. The width ratio and conductivity ratio suppress the flow in both the regions for equal Biot numbers. Similar result was also observed by Prathap Kumar et al. (2009) for isothermal boundary conditions.
5. The Nusselt number at the cold wall was increasing function of $|\varepsilon|$ and decreasing function of σ. The Nusselt number at the hot wall was decreasing function of $|\varepsilon|$ and increasing function of σ.
6. The percentage of error between PM and DTM agree very well for small values of perturbation parameter.
7. Fixing equal values for viscosity, width and conductivity for fluids in both the regions we get back the results of Umavathi and Santosh (2012a,b) for one fluid model.

References

[1] S. Ostrach, "Low-gravity fluid flows," Ann. Rev. Fluid Mech., vol. 14, pp. 313-345, 1982.
[2] W. E. Langlois, "Buoyancy-driven flows in crystal-growth melts," Ann. Rev. Fluid Mech., vol. 17, pp. 191-215, 1985.
[3] D. Schwabe, "Surface-tension-driven flow in crystal growth metals," Crystal. Vol. 11, pp. 848, 1986.
[4] E. M. Sparrow, L. F. A. Azevedo, A. T. Prata, "Two-fluid and single-fluid natural convection heat transfer in an enclosure," ASME J. Heat Transfer, vol. 108, pp. 848-852, 1986.
[5] T. Kimura, N. Heya, M. Tekauchi, H. Isomi, "Natural convection heat transfer phenomenon in an enclosure filled with two stratified fluids," JSME, vol. 52, pp. 617-625, 1986.
[6] G. Beavers, D. D. Joseph, "Boundary conditions at a naturally permeable wall," J. Fluid Mech., vol. 30, pp. 197-207, 1967.
[7] G. Neale, W, Nadar, "Practical significance of Brinkman's extension of Darcy's law: Coupled parallel flows within a channel and a bounding porous medium," Can. J. Chem. Eng., vol. 52, pp. 475-478, 1974.
[8] K. Vafai, S. J. Kim, "Fluid mechanics of the inter-phase region between a porous medium and a fluid layer-an exact solution," Int. J. Heat Fluid Flow, vol. 11, pp. 254-256, 1990.
[9] K. Vafai, R. Thiyagaraja, "Analysis of flow and heat transfer at the interface region of a porous medium," Int. J. Heat Fluid Flow, vol. 30, pp. 1391-1405, 1987.
[10] M. S. Malashetty, J. C. Umavathi, J. Prathap Kumar, "Two fluid flow and heat transfer in an inclined channel containing porous and fluid layer," Heat and Mass Transfer, vol. 40, pp. 871–876, 2004.
[11] M. S. Malashetty, J.C. Umavathi, J. Prathap Kumar, "Flow and heat transfer in an inclined channel containing fluid layer sandwiched between two porous layers," J. Porous Media, vol. 8, pp. 443-453, 2005.
[12] J. C. Umavathi, J. Prathap Kumar, A. J. Chamkha, I. Pop, "Mixed convection in a vertical porous channel," Transport in Porous Media, vol. 61, pp. 315–335, 2005.
[13] J. C. Umavathi, A. J. Chamka, Abdul Mateen, A. Al-Mudhaf, "Oscillatory flow and heat transfer in a horizontal composite porous medium channel," Heat and Technology, vol. 25, 2006.
[14] J. C. Umavathi, A. J. Chamka, Abdul Mateen, A. Al-Mudhaf, "Unsteady oscillatory flow and heat transfer in a horizontal composite porous medium channel," Nonlinear Analysis: Modelling and Control, vol. 14, pp. 397–415, 2009.
[15] J. C. Umavathi, I. C. Liu, J. Prathap-kumar, D. Shaik-meera, "Unsteady flow and heat transfer of porous media sandwiched between viscous fluids," Appl. Math. Mech. Engl. Ed, vol. 31(12), pp. 1497–1516, 2010.
[16] J. C. Umavathi, Jaweriya Sultana, "Mixed convective flow of micropolar fluid mixture in a vertical channel with boundary conditions of third kind," J. Eng. Phys and Thermo Phys, vol. 85, pp. 895-908, 2012.
[17] J. Prathap Kumar, J. C. Umavathi, I. Pop, Basavaraj M. Biradar, "Fully developed mixed convection flow in a vertical channel containing porous and fluid layer with isothermal or isoflux boundaries," Transp. Porous Med., vol. 80, pp. 117–135, 2009.
[18] J. Prathap Kumar, J. C. Umavathi, Basavaraj M. Biradar, "Mixed convection of a composite porous medium in a vertical channel with asymmetric wall heating conditions," Journal of porous medium, vol. 13, pp. 271-285, 2010.
[19] A. K. Al-Hadharami, L. Elliott, D. B. Ingham, "Combined free and forced convection in vertical channels of porous media," Transport Porous Media, vol. 49, pp. 265–289, 2002.
[20] M. Parang, M. Keyhani, "Boundary effects in laminar mixed convection flow through an annular porous medium," ASME J. Heat Transf, vol. 32, pp. 1039–1041, 1987.
[21] K. Muralidar, "Mixed convection flow in a saturated porous annulus," Int. J. Heat Mass Transf, vol. 32, pp. 881–888, 1989.
[22] A. Barletta, E. Magyari, B. Keller, "Dual mixed convection flows in a vertical channel," Int. J. Heat Mass Tranf, vol. 48, pp. 4835–4845, 2005.
[23] A. Barletta, E. Magyari, I. Pop, L. Storesletten, "Mixed convection with viscous dissipation in a vertical channel filled with a porous medium," Acta Mechanica, vol. 194, pp. 123-140, 2007.
[24] P. Wibulswas, "Laminar flow heat transfer in non circular ducts," Ph.D. Thesis, London University, 1966 (as reported by Shah and London in 1971).
[25] R. W. Lyczkowski, C. W. Solbrig, D. Gidaspow, "Forced convective heat transfer in rectangular ducts—general case of wall resistance and peripheral conduction. 1969. Institute of Gas Technology Tech. Info, Center File 3229, 3424S, State, Street, Chicago, Ill 60616 (as reported by Shah and London in 1971).
[26] V. Javeri, "Analysis of laminar thermal entrance region of elliptical and rectangular channels with Kantorowich method," Warme- und Stoffuberragung, vol. 9, pp. 85–98, 1976.
[27] E. Hicken, Das, "Temperaturfield in laminar durchstromten Kanalen mitechteckquerschnitt bei unterschiedlicher Beheizung der Kanalwade," Warme- und Stoffubertragung, vol. 1, pp. 98–104, 1968.
[28] E. M. Sparrow, R. Siegal, "Application of variational methods to the thermal entrance region of ducts," Int. J. Heat Mass Transf, vol. 1, pp. 161–172, 1960.
[29] E. Zanchini, "Effect of viscous dissipation on mixed convection in a vertical channel with boundary conditions of the

third kind," Int. J. Heat and Mass Transf, vol. 41, pp. 3949 – 3959, 1998.
[30] J. C. Umavathi, Santosh Veershetty, "Mixed convection of a permeable fluid in a vertical channel with boundary conditions of a third kind," Heat Transfer Asian Research, vol. 41(6), 2012.
[31] J. C. Umavathi, Santosh Veershetty, **"**Non-Darcy mixed convection in a vertical porous channel with boundary conditions of third kind," Transp Porous Med, vol. 95, pp. 111–131, 2012.
[32] J. C. Umavathi, J. Prathap Kumar, Jaweriya Sultana, "Mixed convection flow in a vertical porous channel with boundary conditions of the third kind with heat source/sink," Journal of Porous Media, vol. 15 (11), pp. 989–1007, 2012.
[33] J. C. Umavathi, J. Prathap Kumar, M. Shekar, "Convective flow between a corrugated and a smooth wall," Journal of Porous Media, vol. 15(10), pp. 975–988, 2012.
[34] M. M. Rashidi, D. D. Ganji, "Homotopy perturbation combined with Pade´ approximation for solving two-dimensional viscous flow in the extrusion process," Int. J. Nonlinear Sci., vol. 7, pp. 387–394, 2009.
[35] O. A. Bég, T. A. Bég, H. S. Takhar, A, Raptis, "Mathematical and numerical modeling of non-Newtonian thermo-hydrodynamic flow in non-Darcy porous media," Int. J. Fluid Mech. Res., vol. 31, pp. 1–12, 2004.
[36] J. K. Zhou, "Differential Transformation and Its Applications for Electrical Circuits," Huazhong University Press, Wuhan, China, 1986 (in Chinese).
[37] Y. L. Yeh, C. C. Wang, M. J. Jang, "Using finite difference and differential transformation method to analyze of large deflections of orthotropic rectangular plate problem," Appl. Math. Comput, vol. 190, pp. 1146–1156, 2007.
[38] A. S. V. Ravi Kanth, K. Aruna, "Solution of singular two-point boundary value problems using differential transformation method," Physics Letters A 372, pp. 4671–4673, 2008.
[39] I. H. Abdel-Halim Hassan, "Application to differential transformation method for solving systems of differential equations," Appl. Math. Mod., vol. 32, pp. 2552–2559, 2008.
[40] M. M. Rashidi, "The modified differential transform method for solving MHD boundary-layer equations," Comp. Phy. Comm, vol. 180, pp. 2210–2217, 2009.
[41] H. Yaghoobi, M. Torabi, "The application of differential transformation method to nonlinear equations arising in heat transfer," Int. Commu. Heat and Mass Transf, vol. 38, pp. 815–820, 2011.
[42] M. Rashidi, O. Anwar Bég, N. Rahimzadehm, "A generalized differential transform method for combined free and forced convection flow about inclined surfaces in porous media," Chem. Eng. Comm, vol. 199, pp. 257–282, 2012.